Chinese Chemical Letters 34 (2023) 108272

Contents lists available at ScienceDirect

Chinese Chemical Letters

journal homepage: www.elsevier.com/locate/cclet

Comparative study of raw and HNO_3-modified porous carbon from waste printed circuit boards for sulfadiazine adsorption: Experiment and DFT study

Yujiao Kan[a], Ruxin Zhang[a,b], Xing Xu[c], Bo Wei[a,d], Yanan Shang[a,*]

[a] School of Safety and Environmental Engineering, Shandong University of Science and Technology, Qingdao 266590, China
[b] Faculty of Light Industry, Qilu University of Technology (Shandong Academy of Sciences), Ji'nan 250353, China
[c] Shandong Key Laboratory of Water Pollution Control and Resource Reuse, School of Environmental Science and Engineering, Shandong University, Qingdao 266237, China
[d] Environment Research Institute, Shandong University, Qingdao 266237, China

ARTICLE INFO

Article history:
Received 13 December 2022
Revised 22 February 2023
Accepted 24 February 2023
Available online 26 February 2023

Keywords:
WPCBs
DFT
Sulfadiazine
Porous carbon

ABSTRACT

A huge amount of waste printed circuit boards (WPCBs) was produced while the electronic manufacturing industry developed rapidly. WPCBs mainly consist of organic compounds, which makes it possible to prepare them into porous carbon as valuable adsorbent. However, WPCBs are also rich in valuable metals. Cu makes up the most of these metals. It is worth studying whether the residual metal will affect the application of carbon materials. In this study, the porous active carbon (AC) was prepared from WPCBs as an adsorbent. Sulfadiazine (SD), a widely detected antibiotic contaminant, was used as a target pollutant. Nitric acid (HNO_3) was used to modify AC (AC-HNO_3) to remove the residual Cu. The experiment results showed that the adsorption kinetics of SD by AC ($k = 0.0025$) and AC-HNO_3 ($k = 0.0029$) can be described better using a *pseudo*-second-order kinetic equation. The adsorption isotherms of AC and AC-HNO_3 on SD could be fitted by the Langmuir model. AC had a larger adsorption capacity than AC-HNO_3. Density functional theory (DFT) calculation results suggested that the −OH group and Cu on the surface of AC could be the adsorption sites and promote the SD adsorption. This work provides practical methods to recycle WPCBs into wealth and realized waste control by waste.

As the electronic manufacturing industry develops rapidly, electronic and electrical equipment is constantly updated, which produces a large number of electronic wastes. In 2025, the total amount of waste printed circuit boards (WPCBs) in China will reach 60 million tons. In the WPCBs, glass fiber is used as the skeleton and epoxy resin is used as the binder to connect the metal copper foil and glass fiber to form a composite material with a complex structure that is difficult to damage under external force [1]. WPCBs are rich in valuable metals, such as Cu, Fe, Al, Sn, Ag, accounting for 30% of WPCBs. It is reported that compared to other metals, Cu has a composition (around 20% of WPCBs) that is notably higher than 10 times that of a natural copper mine [2]. There are many methods to recycle WPCBs, among which the mechanical/physical recycling technique is commonly used in industry. However, a small amount of metal Cu remains in the non-metallic part due to technical limitations in mechanical separation, which hinders the reuse of non-metallic materials.

Since the non-metallic part of the WPCBs is mainly an organic compound, it can be considered as the raw material for preparing carbon materials. In our previous studies, WPCBs can be used to synthesize porous carbon materials by H_3PO_4, NaOH, KOH and steam physical activation method [3–5]. As the raw materials of WPCBs with residual metal copper, the active carbon prepared by steam activation will contain residual metal. It is worth studying whether the residual metal will affect the application of carbon materials.

Antibiotics are organic substances that can specifically block or impact other biological processes even in low quantities [6,7]. Sulfonamides (SM) are common antibiotics that are employed in a variety of areas globally, including medicine, aquaculture, animal husbandry, and others. Sulfadiazine (SD) belongs to sulfonamides [8]. Given the fact that the majority of the SD in water environments or sewage treatment plants is found as ng/L or g/L, it is

* Corresponding author.
E-mail address: shangyanan@sdust.edu.cn (Y. Shang).

https://doi.org/10.1016/j.cclet.2023.108272
1001-8417/

difficult to degrade in the environment and can cause great harm to the human body through biological enrichment [9,10]. The existence of sulfadiazine in the environment may cause the emergence of resistant bacterial strains and damage the organisms of humans and other creatures [11]. Orte *et al.* reported that SD is most toxic toward *Phaeodactylum tricornutum* and *Isochrysis galbana* (two species of marine microalgae) among several chemicals tested [12]. Jin *et al.* reported that sulfadiazine has an inhibiting effect on the growth of wheat roots [13]. At present, there are many methods to remove antibiotic wastewater, among which the adsorption method is widely used on account of its low cost, strong renewable ability, and remarkable removal efficiency. Porous carbon materials as adsorbent have low preparation costs and strong adsorption capacity, so they have been used in wastewater treatment as hot resources in recent years [14].

Herein, nitric acid (HNO_3) was employed to modify WPCBs-based active carbon prepared by the steam method in the early stage. Copper in carbon materials can be removed by modification. The experimental and theoretical calculations were used to study the adsorption effect of the carbon materials before and after modification on sulfadiazine.

The WPCBs were obtained from Zhonglyu Eco-recycle Co., Ltd. (Shandong, China). To obtain the magnetic fraction and non-magnetic fraction, the WPCB powder was first crushed and separated using a grinder, and then the main broken powder was separated using a magnetic separator. The non-magnetic fraction with a size lower than 0.25 mm is raw material. SD (98%) and all the other chemical reagents were purchased from Shanghai Macklin Biochemical Co., Ltd. with analytical grade.

The methods to prepare porous carbon material were carried out with a two-step approach. In the first step, the raw material was carbonized for 2 h at 600 °C in a chamber type electric resistance furnace (KSY-4D-16). After carbonization, the samples were rinsed with deionized (DI) water and then kept at 100 °C for drying. Then, the carbonized sample was activated at 800 °C under a constant steam flow (110 cm^3/min, 0.5 MPa) for 90 min within a horizontal cylindrical furnace (SKQ-3–10). The porous carbon was washed with DI water and kept at 100 °C until dry, smashed, and sieved to obtain a sample with a powder size of 0.15 mm (100 mesh). The sample is named AC. During the HNO_3 modification experiment, 20 g of carbon was mixed and heated in 500 mL of 70% HNO_3 at 70 °C for 24 h Then, the modified porous carbon was filtered out and rinsed with DI water. After verifying that the supernatant was in a neutral pH, the modified porous carbon was dried for 8 h at 100 °C in a dryer. The obtained sample is named AC-HNO_3. The preparation flowchart is presented in Fig. 1a.

The morphology of AC and AC-HNO_3 was studied by a scanning electron microscope (SEM, FEI, NOVA NANOSEM450, USA). The specific surface area and pore size distribution were analyzed using a surface area analyzer (JW-BK122W, Beijing JWGB Sci. & Tech. Co., Ltd., China). The surface chemical functional groups on the samples were examined with Fourier transform infrared spectrum spectroscope (FTIR, 380-Fourier, USA). Density functional theory (DFT) calculation and analysis were conducted by Gaussian 09 [15], MedeA-Vienna Ab initio Simulation Package (VASP) [16], and Multiwfn software (Text S1 in Supporting information) [17]. The adsorption kinetics and adsorption isotherms were obtained by batch adsorption tests (Text S2 in Supporting information).

Fig. 1b presents the nitrogen adsorption-desorption isotherms of AC and AC-HNO_3 with the characteristics of Type I and Type IV. At low pressure, isotherm shows Type I, which suggested that there were a lot of micropores in the material. The hysteresis loop at high pressure indicates that there was capillary condensation, indicating that the material had rich mesopores. The hysteresis loop was within the range of 0.4∼1.0, suggesting that the mesopores were widely distributed. It can be seen from Fig. 1c and Table S1 (Supporting information) that both AC and AC-HNO_3 had micropores, mesopores and a few macropores, but mostly micropores. AC had a high microporous volume and a large specific surface area. After being modified by HNO_3, the amorphous microporous and graphite microcrystals formed on the surface of carbon materials were corroded. As a result, the microporous were gradually expanded and transformed into mesoporous, resulting in a 54.5% of reduction in the surface area and a 57.4% of reduction in the pore volume.

The FT-IR spectra of AC and AC-HNO_3 are presented in Fig. 1d. The characteristic peaks at 2924 cm^{-1} and 2425 cm^{-1} are caused by the vibration stretching of the C-H bond and O-H bond, respectively [18]. The peaks at the binding energy of 1650 cm^{-1} and 1529 cm^{-1} are assigned to the carbon-oxygen double bond (C=O) and a carbon-carbon double bond (C=C) stretching vibration [19]. The peaks at 1400 cm^{-1} and 1090 cm^{-1} correlates to the stretching vibration of CH_3 and SO_3 groups, respectively [20]. The characteristic peak of the P-Cl group appears at 490 cm^{-1} [21]. After modification with nitric acid, C=O and CH_3 groups disappeared, indicating that these chemical bonds were broken and the content of the O element decreased. Meanwhile, the signal of the C = C group increased, which indicated that more π-π bonds existed in AC-HNO_3. AC and AC-HNO_3 have similar infrared spectral bands, but the absorption peak intensity of AC is smaller than that of AC-HNO_3, which may be due to the distinguishing element contents of the two carbon materials.

Figs. 1e and f display the SEM images of AC and AC-HNO_3. The activated carbon surface before modification is relatively rough. AC has a pore structure, but the pore structure distribution is irregular, and the size is different. This was because the organic substances in WPCBs volatilize under the high carbonization temperature, and a rich pore structure was formed under the secondary activation of water vapor. AC has some small particles attached to its surface. Combined with the composition of WPCBs, it was analyzed that these particles were copper particles condensed by high-temperature heating from the residual copper in the process of WPCB sorting. Compared with the AC, AC-HNO_3 shows an obvious layered structure, and the copper particles disappeared. This suggested that the metal copper was dissolved when it was modified by nitric acid. The elemental composition of AC and AC-HNO_3 surfaces was analyzed by an energy spectrum analyzer (Fig. S1 in Supporting information). The content of elements of the samples changed obviously before and after modification, and the content of C increased from 28.67% to 89.51%. O element dropped from 25.94% to 10.23%. Si decreased from 4.12% to 0.21%. The content of Cu decreased from 49.51% to 0.05%. The decrease of Cu indicated that the residual copper in WPCBs was removed by nitric acid modification.

The adsorption kinetics of SD by AC and AC-HNO_3 are examined using the *pseudo*-first-order and the *pseudo*-second-order kinetic model (Text S3 in Supporting information). Adsorption kinetic is presented in Fig. S2 (Supporting information). The linear fitting results are presented in Figs. 2a, b and Table S2 (Supporting information). The first step of the adsorption reaction can be better described by the *pseudo*-first-order kinetic equation. But, as the adsorption reaction proceeds, the adsorption data gradually deviates from the fitting curve. The *pseudo*-second-order kinetic equation provides a more accurate description of the adsorption of SD by AC and AC-HNO_3 ($R^2 > 0.99$). The *pseudo*-first-order kinetic equation is generally applied to describe the adsorption kinetics with a relatively single process. Surface adsorption and internal diffusion are just two of the adsorption processes that are included in the *pseudo*-second-order kinetic model. Consequently, the adsorption procedures were complicated. In the *pseudo*-second-order kinetic equation, the adsorption rate constants (k) are 0.0025 and 0.0029, respectively, showing that the adsorption rate of AC-HNO_3

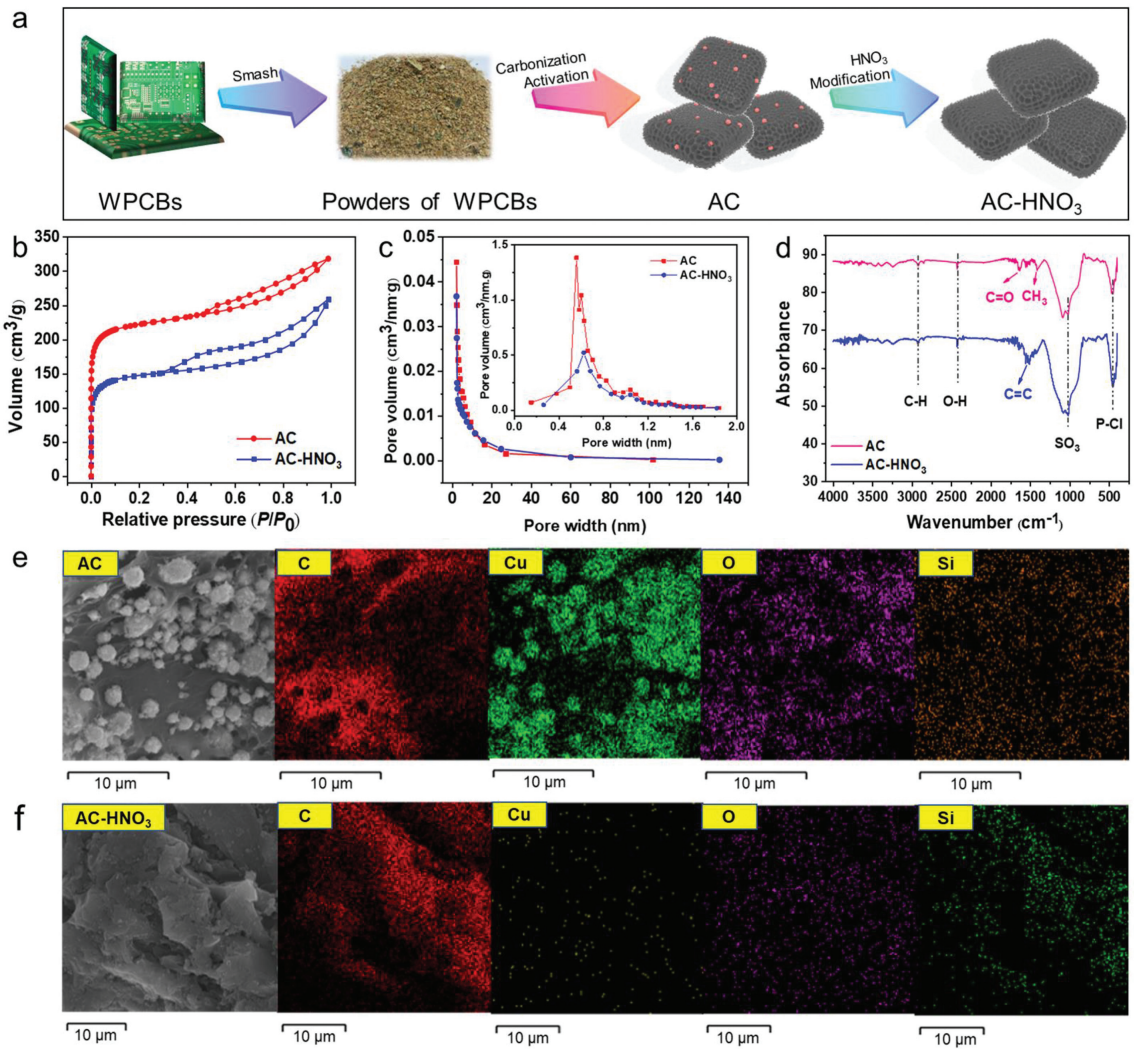

Fig. 1. (a) Synthesis mechanism diagram for AC and AC-HNO_3. (b) Nitrogen adsorption-desorption isotherms, (c) pore size distribution curve and (d) FTIR spectra of AC and AC-HNO_3. SEM and corresponding EDS mapping of (e) AC and (f) AC-HNO_3.

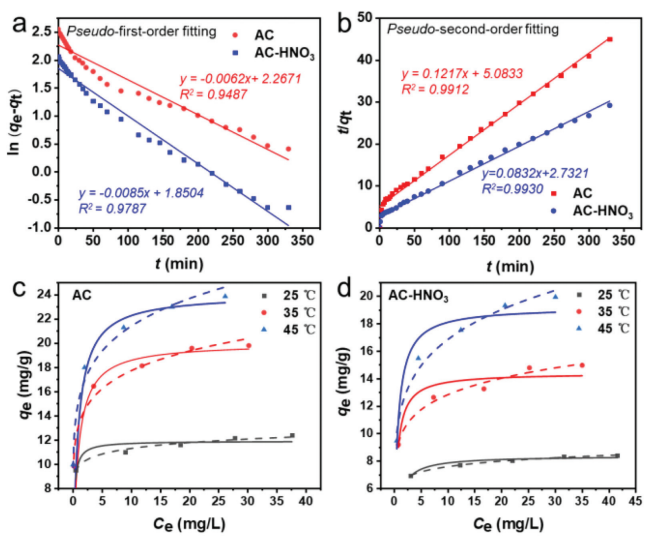

Fig. 2. Linear fitting results of (a) *pseudo*-first-order and (b) *pseudo*-second-order kinetic model of SD adsorption by AC and AC-HNO_3 ([SD] = 40 mg/L, adsorbent dosage = 1 g/L). Adsorption isotherms of SD on (c) AC and (d) AC-HNO_3 (adsorbent dosage = 1 g/L).

for SD was faster, while chemical adsorption may occur during the adsorption of SD.

The adsorption isotherms of AC and AC-HNO_3 on SD at 25, 35 and 45 °C are shown in Figs. 2c and d. The data were fitted with Langmuir and Freundlich models (Text S4 in Supporting information). The fitting data are shown in Table S3 (Supporting information). SD adsorption capacity of the carbon adsorbent is higher before modification. The maximum adsorption capacity of the Langmuir model for AC at 25 °C is 12.79 mg/g, while AC-HNO_3 reduces to 8.37 mg/g. At 25 °C, the coefficients R^2 of the Langmuir model are 0.9442 and 0.9197. The fitting coefficients of Freundlich are 0.9897 and 0.9951, which are higher than that of the Langmuir model. Therefore, the fitting result of the Freundlich model is better than the Langmuir model. K_f of the Freundlich model is a constant positively related to adsorption capacity. As can be seen from Table S3, K_f gradually increases with the rise of temperature, and the adsorption capacity of AC is greater than that of AC-HNO_3. The values of 1/n in the Freundlich model are all less than 1, indicating that these two carbon adsorbents are favorable for SD adsorption.

DFT calculation was used for a better understanding of the adsorption mechanism. The possible configurations of AC and AC-HNO_3 were optimized by DFT (Fig. S3 in Supporting information). Electrostatic potential (ESP) is a useful method to show the state of atoms in a certain configuration [22]. As shown in Figs. 3a-c,

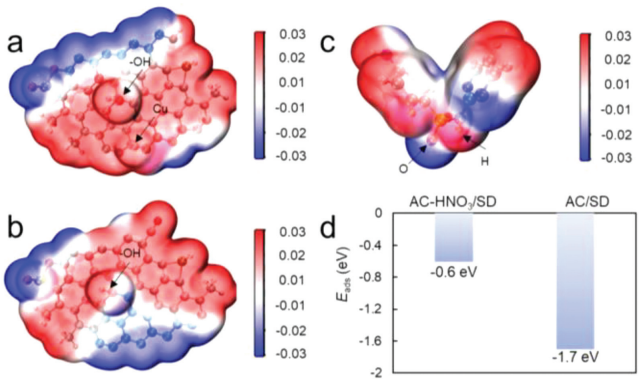

Fig. 3. ESP of the possible structure of (a) AC, (b) AC-HNO_3, and (c) SD; (d) adsorption energy of AC-HNO_3/SD and AC/SD.

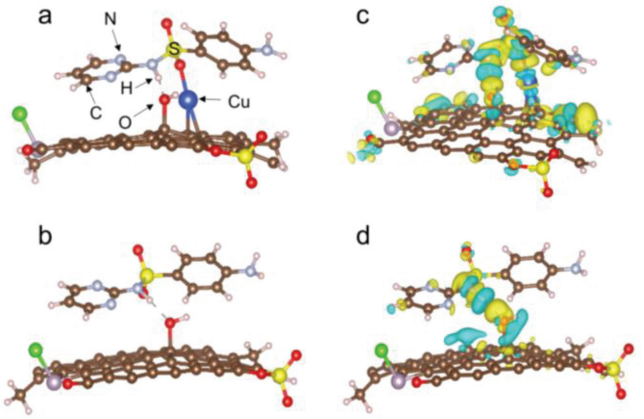

Fig. 4. Configurations of SD adsorbed on (a) AC and (b) AC-HNO_3. (c, d) Corresponding differential charge density (yellow isosurfaces represent regions of electron accumulation and blue isosurfaces represent regions of electron loss).

the colors red and blue are employed to represent the positive and negative electrostatic potential energy values, respectively. Fig. 3a shows that the Cu atom in the carbon support presented a positive charge, which could be an adsorption site to combine with the negative site of the adsorbate. However, without the Cu atom, the surface of the configuration tended to be negative (Fig. 3b). The ESP of SD is presented in Fig. 3c, which suggested that the O atoms bonded to the S atom in SD were negative charges. Hence, the O atoms in SD could easily be adsorbed on the Cu site of AC. The adsorption energy (E_{ads}) of the SD adsorbed on AC and AC-HNO_3 indicated that AC had higher E_{ads} than AC (-1.7 eV *vs.* -0.6 eV) (Fig. 3d). This also suggested that AC had stronger adsorption ability than AC-HNO_3.

Configurations of SD adsorbed on AC and AC-HNO_3 were optimized by DFT and presented in Fig. 4. As can be seen, the O atoms of SD combined with Cu had a bond. Besides, the H atom in SD tended to combine with the −OH group on the AC and AC-HNO_3 to form a hydrogen bond. The diagrams of differential charge density show that electrons drifted to the middle of the H−O and Cu−O bond, which suggested the −OH and Cu could be the adsorption sites [23].

In summary, the AC prepared from the WPCBs can be an efficient adsorbent for SD removal. HNO_3 modification reduced the surface functional groups and Cu elements on the carbon adsorbent. Besides, the total pore capacity and specific surface area can also be greatly reduced. Hence, the adsorption capacity towards SD deceased. This work provided practical methods to recycle WPCBs into wealth and realized waste control by waste.

Declaration of competing interest

The authors declare that they have no known competing financial interests or personal relationships that could have appeared to influence the work reported in this paper.

Acknowledgments

This work was supported by the Natural Science Foundation of Shandong Province Youth Project (No. ZR2021QE208).

Supplementary materials

Supplementary material associated with this article can be found, in the online version, at doi:10.1016/j.cclet.2023.108272.

References

[1] T. Huang, J. Zhu, X. Huang, et al., Waste Manag. 139 (2022) 105–115.
[2] S.X. Shi, S.Q. Jiang, C.C. Nie, et al., Process. Saf. Environ. 166 (2022) 123–132.
[3] Y. Kan, Q. Yue, J. Kong, et al., Chem. Eng. J. 260 (2015) 541–549.
[4] Y. Kan, Q. Yue, B. Gao, et al., J. Taiwan Inst. Chem. Eng. 68 (2016) 440–445.
[5] Y. Kan, Q. Yue, B. Gao, et al., Mater. Lett. 159 (2015) 443–446.
[6] Q. Wang, Q. Xue, T. Chen, et al., Chin. Chem. Lett. 32 (2021) 609–619.
[7] K. Deng, Y. Li, X. Liang, et al., Chin. Chem. Lett. 33 (2022) 1619–1622.
[8] X. Xiang, L. Wu, J. Zhu, et al., Chin. Chem. Lett. 32 (2021) 3215–3220.
[9] Z.L. Li, D. Cao, H. Cheng, et al., Chin. Chem. Lett. 33 (2022) 2747–2752.
[10] C. Lyu, L. Zhang, D. He, et al., Chin. Chem. Lett. 33 (2022) 930–934.
[11] B. Bojarski, B. Kot, M. Witeska, Pharmaceuticals 13 (2020) 189.
[12] M.R. de Orte, C. Carballeira, I.G. Viana, et al., Chem. Ecol. 29 (2013) 554–563.
[13] C.X. Jin, Q.Y. Chen, R.L. Sun, et al., Ecotoxicology 18 (2009) 878–885.
[14] Y. Gao, Q. Wang, G. Ji, et al., Chem. Eng. J. 429 (2022) 132387.
[15] M.J. Frisch, G.W. Trucks, H.B. Schlegel, et al., Gaussian 09, Revision E.01, Gaussian, Inc., Wallingford CT, 2009.
[16] G. Kresse, J. Furthmüller, Comput. Mater. Sci. 6 (1996) 15–50.
[17] T. Lu, F. Chen, J. Comput. Chem. 33 (2012) 580–592.
[18] I.F. Myronyuk, V.I. Mandzyuk, V.M. Sachko, et al., Nanoscale Res. Lett. 11 (2016) 508.
[19] S.Y. Lin, M.J. Li, Y.S. Wei, Spectrochim. Acta A 60 (2004) 3107–3111.
[20] R.L. Frost, W.N. Martens, L. Rintoul, et al., J. Raman Spectrosc. 33 (2002) 252–259.
[21] B.K. Ystenes, Vib. Spectrosc. 17 (1998) 117–121.
[22] P.C. Rathi, R.F. Ludlow, M.L. Verdonk, J. Med. Chem. 63 (2020) 8778–8790.
[23] B. Wei, W. Wang, J. Sun, et al., Appl. Surf. Sci. 511 (2020) 145549.